www.ietdl.org

Published in IET Microwaves, Antennas & Propagation
Received on 8th June 2011
Revised on 4th August 2011
doi: 10.1049/iet-map.2011.0269

ISSN 1751-8725

Reduced-size circularly polarised square microstrip antenna for 2.45 GHz RFID applications

D.L. Nguyen K.S. Paulson N.G. Riley

Department of Engineering, University of Hull, Hull, Yorkshire, UK
E-mail: n.g.riley@hull.ac.uk

Abstract: This study proposes a new design of circular polarised (CP), microstrip (patch) antenna using a set of slits and slots to effectively reduce the area of patch by 67% compared with the conventional, corner truncated, circular polarised square patch. The antenna is designed to operate at 2.45 GHz in the Industrial-Scientific-Medical (ISM) band and has many applications in short-range data communications such as in wireless sensors, radio frequency identification and personal area networking. The proposed antenna has been simulated using HFSS. The design has been fabricated and an extensive measurement campaign has confirmed simulation results. The proposed antenna has a low bore-sight axial ratio of 0.77 dB and a 10 dB bandwidth of 70 MHz. The overall antenna size is 19.6 mm × 19.6 mm on a substrate of thickness 1.59 mm. A second design with a more complex network of slots and slits achieves similar performance in simulation with an overall side length of 13.2 mm, but at the cost of a much larger input impedance.

1 Introduction

Radio frequency identification (RFID) systems operating in the microwave, industrial-scientific-medical (ISM) bands have many applications, as they provide fast tag reading over useful distances. The ISM bands are defined by the International Telecommunication Union, Radiocommunication Sector (ITU-R) in 5.138, 5.150 and 5.280 of the radio regulations, and a range of active and passive RFID systems use the ISM frequency 2.45 GHz. Typically, RFID systems consist of the reader and many tags attached to items. Readers are aware that a particular tag is within its read range, but provide no further information on its location. Currently, research effort is addressing this problem using phased arrays of antennas to implement software-controlled scanning of the volume monitored by the reader. A single reader could provide the direction to a particular tag. Range could be derived from receive power levels. Alternatively, two readers could determine tag position by triangularisation. The size of both tags and readers is limited by the antenna size. Although tag antennas are usually linearly polarised, reader antenna need to be circularly polarised (CP) to reduce sensitivity to tag orientation. For these reasons, the development of compact, CP antennas is important to extend the miniaturisation, applications and use of microwave RFID systems in logistics, and supply chain management.

The first microstrip antenna was introduced in the 1950s [1]. Microstrip antennas have many advantageous characteristics such as a low profile, compactness, light weight and ease of fabrication either alone or with microwave circuits, particularly monolithic microwave integrated circuits. For these reasons, microstrip antennas have become ubiquitous in microwave radio communications systems. A CP antenna with a single microstrip-line feed is one of the simplest radiators for exciting circular polarisation. They are more compact than dual fed antennas [2]. However, as antennas are made smaller, it becomes more difficult to maintain performance, particularly the circular polarisation, across the required RFID bandwidth of 83.5 MHz.

In 1983, Sharma and Gupta [3] introduced a square patch (SP) antenna with symmetric-corner truncations to produce CP. These perturbations generate two orthogonal modes of the same amplitude but quadrature in phase. Many designs of single-feed, CP, SP antennas have been reported since and a review is available in [4]. Developments in the last decade have focused on miniaturisation of SP antennas by the introduction of symmetrical patterns of holes within the patch. These force greater meandering in the fundamental-mode current paths and so the patch size can be reduced while maintaining the resonant frequency. Examples include those of [5, 6]. More recently, asymmetric designs have been proposed, such as square patches with asymmetric patterns of circular holes, for example, Nasimuddin *et al.* [7].

In this document, we propose several new designs of CP and SP antennas. These designs incorporate the two truncated corners of Sharma and Gupta to produce CP. In addition, a regular pattern of slits and slots forces greater meandering and so allows for smaller overall antenna size. Section 2 introduces the first design that achieves an area reduction of 67% compared to the conventional CP, corner-truncated SP without slits and slots. The area reduction is more than other published designs including the square ring method (size reduction of 19% [8]), square ring and a slit (size reduction of 19% [9]), slits (size reduction of 36% [5] or 55% [10]) and asymmetric circular slots with and without slits (size reduction of about 10 and 22% [7]). In Section 3, a matched transformer feed is developed so the antenna can be driven by a standard 50 Ω line. The proposed compact CP antenna design is simulated and antenna characteristics are verified by measurements performed on fabricated antennas. These are described in Section 4. Section 5 discusses the limits of antenna miniaturisation using slits and slots.

2 Antenna design

This section describes the design of two antennas, a standard truncated corner and a novel antenna with the addition of slits and slots. The antennas are initially designed using heuristics and then the designs are modelled with a commercial, electromagnetic field, finite element modelling package (HFSS). The modelling allowed the geometry of the designs to be adjusted to ensure the same fundamental resonant frequency and to optimise other figures of merit such a axial ratio and return loss bandwidths.

For all antenna design and fabrication, an FR4 substrate was used. This has a thickness of 1.59 mm, relative permittivity $\varepsilon_r = 4.1$ and dielectric loss tangent $\tan\delta = 0.02$. These parameters were determined by measurement. Antennas were fabricated on rectangles of FR4 substrate of dimensions: 100.00 × 70.00 × 1.59 (length × width × thickness in millimetre).

A truncated corner, CP–SP antenna was designed. The edge length, a, of such an antenna is typically slightly smaller than half the wavelength of the fundamental resonant frequency. The corner truncation size c of this antenna is approximately related to the patch edge length a by the following equation

$$\frac{c}{a} = \sqrt{\frac{1}{2Q_0}} \quad (1)$$

where Q_0 the unloaded quality factor representing antenna losses.

This antenna, fed by a quarter wave transformer, was simulated using commercial HFSS simulation software and the values of c and a estimated using (1) were refined to impose the resonant frequency of 2.45 GHz. The resulting dimensions are listed in Table 1 (Antenna A).

The proposed design of compact, corner truncated, CP and SP antenna using four identical pairs of slits and a cross slot at the centre is shown in Fig. 1. The patch is defined by a set of dimensions of a, c, x_1, y_1, y_2, w and x_2. The effect of varying these parameters on performance has been investigated by simulation.

The proposed design, optimised for a resonant frequency of 2.45 GHz, has a patch size of $a = 19.60$ mm and the truncated corners' length of $c = 1.70$ mm. Each slit is 6 mm long and 1 mm wide and the two slits in a pair are separated by 4.0 mm ($x_1 = 6.0$ mm, $y_1 = 6.0$ mm and $y_2 = 4.0$ mm). The cross slot has width of $w = 1.0$ mm and length of $x_2 = 10.0$ mm.

The combination of slits and slots effectively increases the length of the current streamlines associated with the fundamental mode of excitation. Consequently the fundamental frequency is lower than for a similar antenna without slots. Therefore for the same resonant frequency, the proposed antenna can be smaller than the conventional design.

The size reduction is determined by the dimensions of the slits and slot. For the design described above, the patch edge length a approximately one-third smaller than the conventional corner-truncated CP and SP with an edge length of 29.50 mm.

The antenna excites right-hand CP or left-hand CP radiation depending on the antenna feeding position on the X- or Y-axis.

3 Matching to feed transmission line

Many patch antennas are driven by coaxial cable at the chosen point to match the antenna input impedance to the characteristic impedance of the cable. For patch antennas to be integrated into RF systems, it is more desirable for the antenna to be driven by a microstrip transmission line that joins the patch at the edge. To optimise power transmission to the antenna, some system is required to match the antenna to the microstrip.

The proposed antenna configuration has been simulated using HFSS software to obtain the input impedance at the antenna edge, on the X-axis. The antenna input impedance has been calculated to be

$$Z_a = 209.52 - j52.31\Omega \quad (2)$$

The antenna may be matched to 50 Ω port using a generalised transformer, that is, a short section of new transmission line is inserted between the main 50 Ω transmission line and the load. The characteristic impedance Z_t line can be estimated using (3). Once Z_t is known, the length of the transformer l can be estimated using (4),

Table 1 Dimensions and measured parameters for the three antennas A, B, and C

Antennas	A: conventional	B: proposed	C: optimised
Dimensions			
patch size (a), mm	29.50	19.60	16.80
length of slits (x_1), mm	–	6.00	4.80
cross slot length (x_2), mm	–	10.00	15.00
truncation size (c), mm	3.30	1.70	1.62
Measured values			
resonant frequency, GHz	2.45	2.47	2.47
AR, dB	0.58	0.93	0.99
return loss	27.08	26.28	25.44
bandwidth of 10-dB return loss, %	4.08	2.85	2.65
gain, dBi	7.0	6.73	6.6

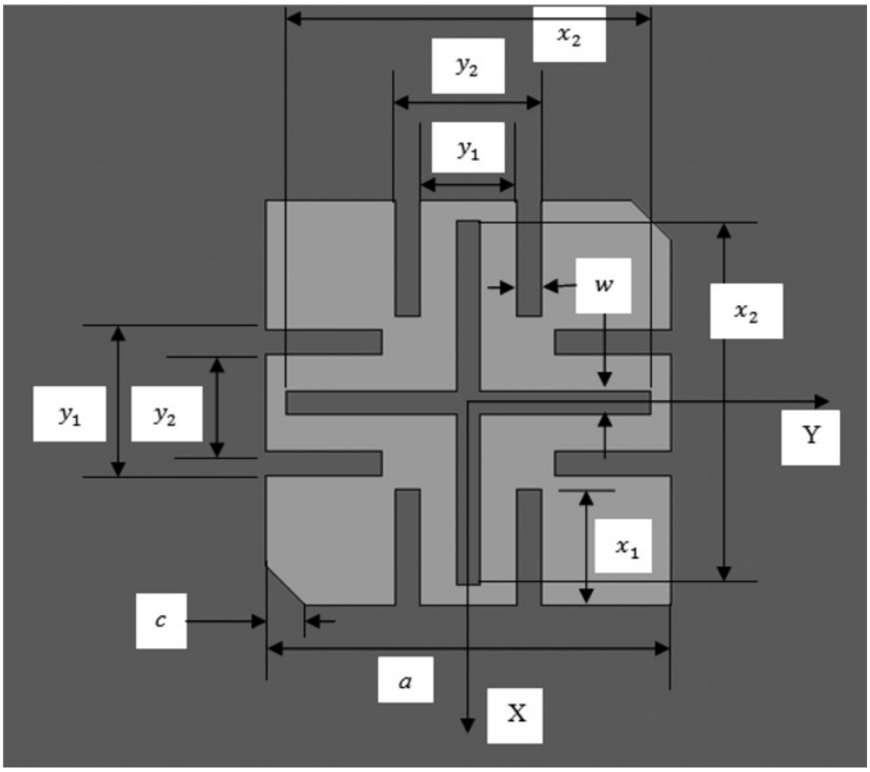

Fig. 1 *Proposed antenna configuration*

where β is the wave number of the travelling wave

$$Z_t = \frac{\sqrt{Z_0 R_A - R_A^2 - X_A^2}}{\sqrt{1 - (R_A/Z_0)}} \quad (3)$$

$$\tan(\beta l) = \frac{Z_t(Z_0 - R_A)}{Z_0 X_A} \quad (4)$$

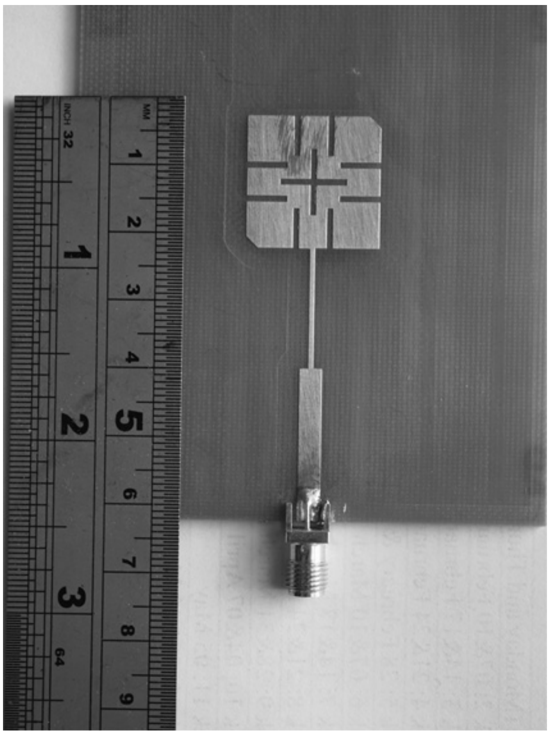

Fig. 2 *Fabricated proposed antenna*

In (3) and (4), the characteristic impedance of the driving line is $Z_0 = 50\ \Omega$ and the input impedance of the antenna is $Z_A = R_A + jX_A$.

The transformer dimensions are estimated using (3) and (4), and then refined using HFSS software simulation. Fig. 2 illustrates the fabricated antenna with the matching transformer line. The transformer's length and width are 17.9 mm and 0.7 mm, respectively, compared to the $Z_0 = 50\ \Omega$ strip width of 3.2 mm.

4 Comparison of simulated and measured characteristics

The proposed antenna and matched feed have been modelled and simulation results have been verified by measurements performed on an antenna in a shielded room. The antenna (Fig. 2) with matching network was simulated using Ansys's HFSS 11, which uses finite-element modelling of Maxwell's equations within a volume with a boundary assumed to be totally absorbing. The antenna was fabricated by a milling process on double-sided, copper, FR4 substrate. A ground plane covers the opposite side.

The simulation predicted a fundamental resonant frequency of 2.455 GHz (where the return loss is 27.51 dB). The bandwidth for a return loss 10 dB lower, that is, VSWR = 1.93 is about 60 MHz or 2.45% of the design resonant frequency. These figures agree well with the measured characteristics. Fig. 3 shows the measured reflection coefficient (S_{11}) displayed on the Agilent E8358A Network Analyzer over the frequency range 1–3 GHz. The measured resonant frequency is 2.470 GHz with a return loss of 26.28 dB. The bandwidth for a reflection coefficient of −10 dB is about 70 MHz or 2.85%. The differences from the simulation results are because of limitations in the uniformity and estimation of the relative permittivity of the substrate and simulation errors because of the limited

IET Microw. Antennas Propag., 2012, Vol. 6, Iss. 1, pp. 94–99
doi: 10.1049/iet-map.2011.0269

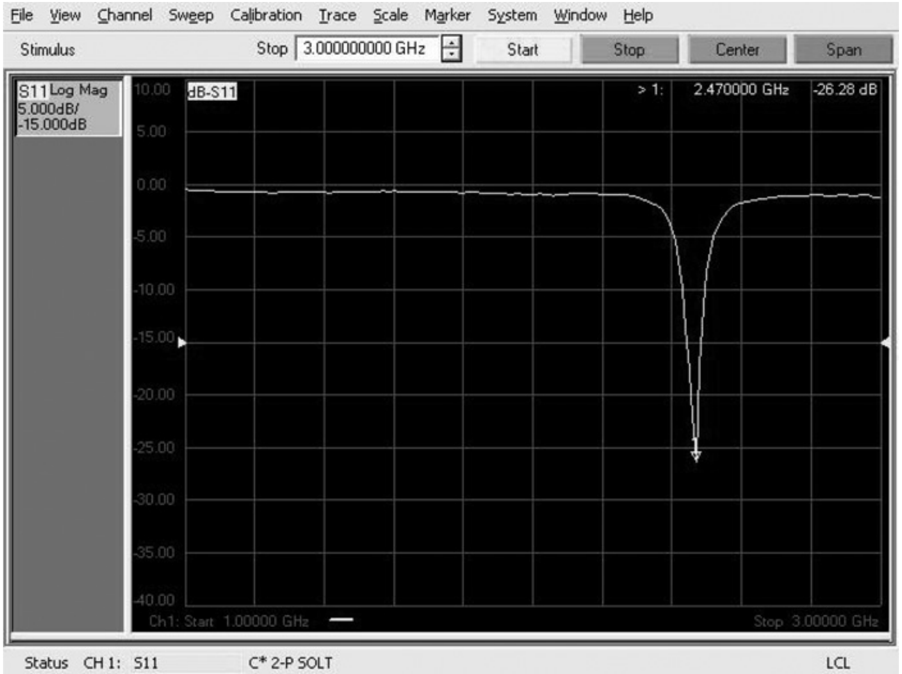

Fig. 3 *Measured reflection coefficient (S_{11}) showing minimum of −26.28 dB at 2.47 GHz*

volume of simulation, the boundary conditions and the number of finite elements.

Fig. 4 shows the current distribution on the patch surface. The lowest current densities are located at the patch corners. The strongest currents are around the end of the slot and slits. It shows that the surface current path is effectively lengthened by the slot and slits resulting in lower resonance frequency.

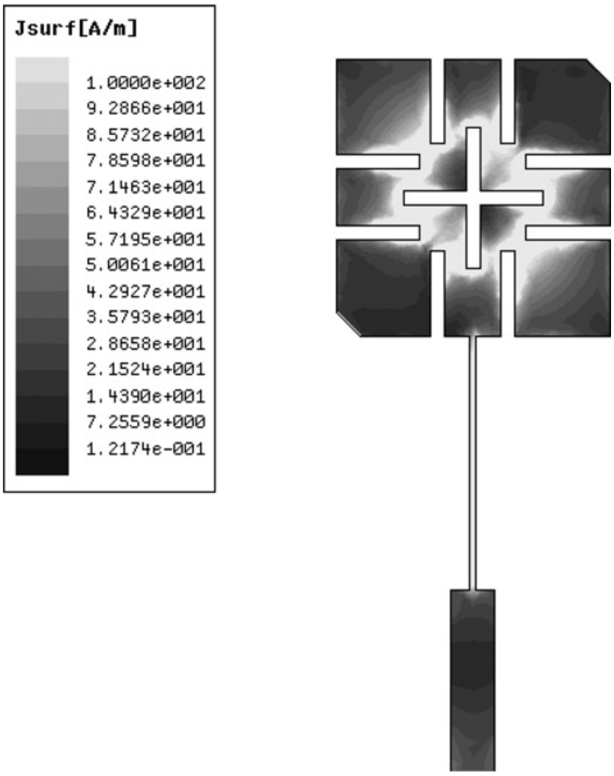

Fig. 4 *Simulated patch surface current magnitude distribution (J_{surf}) of phase 0 at 2.45 GHz*

A measure of the quality of the CP field radiated is the axial ratio, see (5). AR is the ratio of major and minor axes of the polarisation along the bore-sight for the proposed antenna, derived either from the simulation or measured on the fabricated antenna

$$\mathrm{AR[dB]} = 20 \ \log \frac{E_{max}}{E_{min}} \tag{5}$$

Fig. 5 shows the simulated and the measured AR along the bore-sight. The CP bandwidth of the simulated antenna, determined from 3 dB AR, is about 20 MHz, that is, about 0.8% of the designed centre frequency of 2.45 GHz. The simulation also shows that at 2.45 GHz the AR along the bore-sight is minimal, that is, $\mathrm{AR}_{min} = 0.77$ dB.

The AR was measured by using a linearly polarised horn antenna that was rotated in the plane normal to the direction of the incident field in the RF shielded room of Department of Engineering, University of Hull, UK. The beamwidths for circular polarisation AR < 3 dB in XZ-plane $\phi = 0^\circ$

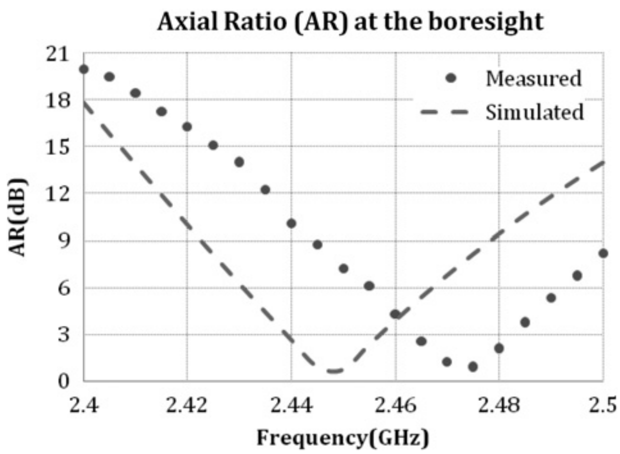

Fig. 5 *Axial ratio (AR) of the designed antenna at the bore-sight*

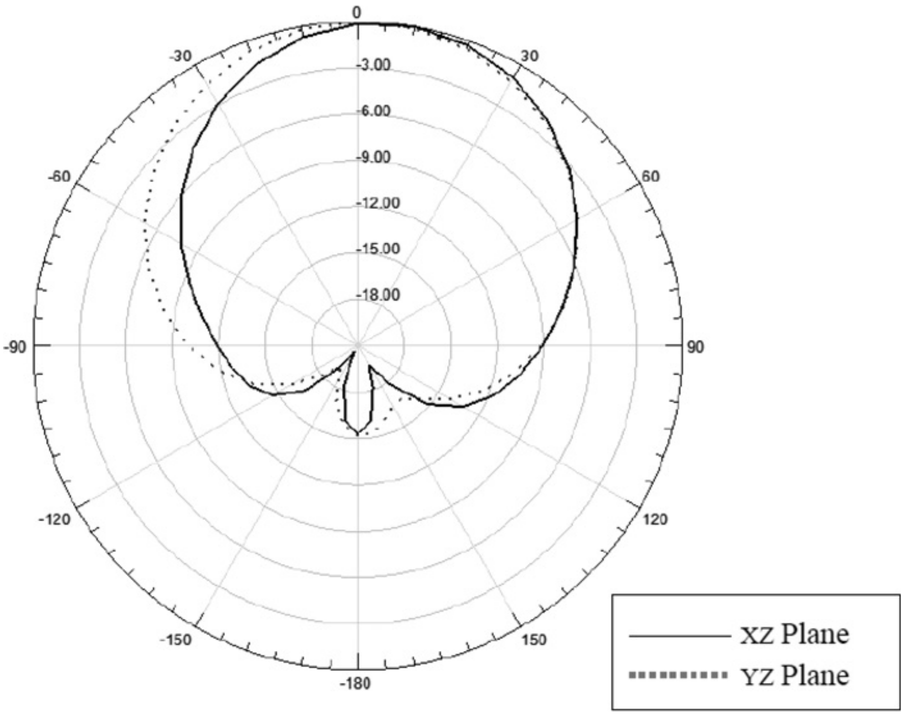

Fig. 6 *Radiated power relative to bore-sight direction, measured on the fabricated antenna*

plane) and in YZ-plane $\phi = 90^{\circ}$ plane) are shown to be approximately 70° both simulation and measurement.

The antenna's radiation pattern was measured and the normalised pattern is illustrated in Fig. 6. The measured half-power beamwidths in XZ- and YZ-plane are 80° and 90°, respectively. The maximum directivity in YZ-plane, as calculated from the measured data, is 6.59 dB at broadside direction, and in XZ-plane is 6.73 dB at an angle of $\theta = 10^{\circ}$.

5 Size optimisation and proposal for a more compact size reduced antenna

In this section, the patch size length a is minimised by modifying the length of cross slot x_2, the length of slits x_1 and the corner truncation size c to maintain circular polarisation. First of all, the proposed antenna was modified by maximising the length of slots and slits. Simulation results show that the modified antenna works at a frequency of about 2.05 GHz, that is, 83.7% of the designed frequency. It implies that the size of an antenna resonant at 2.45 GHz would be about 16.5 mm. A series of models of corner truncated, CP and SP antennas with edge feeds have been simulated. A brute-force search of the (x_1, x_2, c) parameter space was performed to identify antennas (with appropriate matching networks), which matched a range of constraints on resonant frequency, AR and return loss, with patch sizes centred on 16.5 mm and varied in steps of 0.1 mm. Refined brute-force searches were performed in the parameter space regions identified as containing optimal solutions. The parameters of antenna C (see Table 1) were identified to yield a minimum area antenna with a resonant frequency of 2.45 GHz.

The optimised antenna has size length of $a = 16.80$ mm. This antenna and its matched feed have been fabricated and are illustrated in Fig. 7.

Antenna A is the standard design without slots. Antenna B is the proposed design with dimensions shown in Section 2. Antenna C is optimised for minimum patch size at a

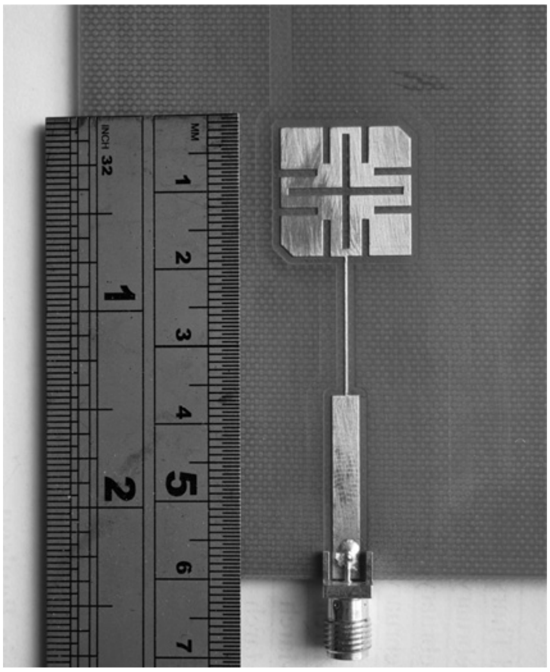

Fig. 7 *Optimised antenna C*

frequency of 2.45 GHz. Table 1 lists the dimensions defining each antenna, that is, the edge length (a), the truncated corner length (c), the slits length (x_1) and the cross slot length (x_2). Measured values of resonant frequency, AR and return loss are also listed in Table 1 for each antenna.

Comparing antennas A and B, the proposed antenna is smaller, that is, the patch edge length has been reduced by approximately 33.56% and the area has reduced by 55.85%. The optimised antenna C (see Fig. 7) with the longer cross-slot of 15 mm has the smallest patch size length because of greatest meandering forced onto the current streamlines.

doi: 10.1049/iet-map.2011.0269

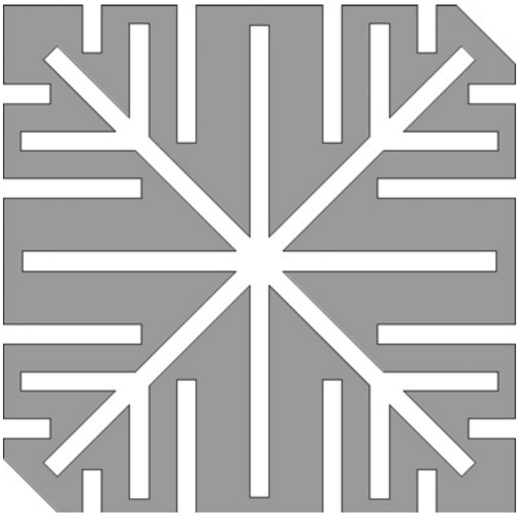

Fig. 8 *Improved design*

The optimised design, antenna C (with parameters shown in Table 1), achieves a reduction of 43.05% in patch length or 67.56% in area compared to conventional design A.

Optimised antenna C has similar radiation pattern to antenna B. Their gains are smaller than the conventional one. This has been verified by measured gains of these antennas (6.6 dBi compared to 7.0 dBi).

Moreover, because of the high reactive impedance at the edge, the microstrip feeding technique using generalised matching may not be suitable. As the characteristic impedance of the line becomes very large, the resulting transformer line is very thin and may not supply enough power to the antenna.

As the current streamlines are forced into more complex meanders, the antennas become smaller but the input impedance increases. The antenna illustrated in Fig. 8 can be generalised into a snowflake design with a large number of slots and slits. The design in Fig. 8 yields an antenna with an area only 20% that of the standard CP and SP with no slots or slits. However, the input impedance at the edge has an extremely large reactive component ($Z_{edge} = 360.70 - j346.92\ \Omega$) so the generalised matching technique is not suitable. Other matching techniques could be used, such as single or double stub matching. The success of matching becomes critically dependent upon the exact geometry and electrical properties of the stubs.

6 Conclusions

In this paper, several new compact CP, microstrip, and SP antennas have been proposed. They have been designed for RFID systems operating in the ISM band around 2.45 GHz. Simulated and measured results show that the proposed antenna yields sufficient circularly polarised radiation at the target frequency. These antennas yield significant miniaturisation compared to a conventional, corner truncated, CP and SP antenna operating at the same frequency, and compared to other published solutions. The proposed design has a simple structure, can be fabricated at low cost, and provides good performance across the narrow target bandwidth. The antenna maybe suitable for use in steerable phased arrays. In conclusion, this type of antenna may prove very suitable for many applications that work within narrow bandwidths, particularly in RFID applications.

7 Acknowledgment

The authors thank Mr S. Coopland, from Electronics Workshop of The University of Hull, for his assistance during the prototyping.

8 References

1 Deschamps, G.: 'Microstrip microwave antennas'. Proc. Third USAF Symp. on Antennas, October 1953
2 Pozar, D.M., Duffy, S.M.: 'A dual-band circularly polarized aperture-coupled stacked microstrip antenna for global positing satellite', *IEEE Trans. Antennas Propag.*, 1997, **45**, (11), pp. 1618–1624
3 Sharma, P.C., Gupta, K.C.: 'Analysis and optimized design of single feed circularly polarized microstrip antennas', *IEEE Trans. Antennas Propag.*, 1983, **29**, pp. 949–955
4 Garg, R., Bhartia, P., Bahl, I., Ittipiboon, A.: 'Microstrip antenna design handbook' (Artech House Inc., 2001)
5 Chen, W.S., Wu, C.K., Wong, K.L.: 'Novel compact circularly polarized square microstrip antenna', *IEEE Trans. Antennas Propag.*, 2001, **49**, (3), pp. 340–342
6 Row, J.S., Ai, C.Y.: 'Compact design of single-feed circularly polarized microstrip antenna', *Electron. Lett.*, 2004, **40**, (18), pp. 1093–1094
7 Nasimuddin, Chen, Z.N., Qing, X.: 'Asymmetric-circular shaped slotted microstrip antennas for circular polarization and RFID applications', *IEEE Trans. Antennas Propag.*, 2010, **58**, (12), pp. 3821–3828
8 Chen, W.S., Wu, C.K., Wong, K.L.: 'Single-feed square-ring microstrip antenna with truncated corners for compact circular polarization operation', *Electron. Lett.*, 1998, **34**, (11), pp. 1045–1047
9 Chen, W.S., Chen, H.D.: 'Single-feed circularly polarized square-ring microstrip antennas with a slit'. IEEE Antennas and Propagation Society Int. Symp., 1998, vol. 3, pp. 1360–1363
10 Chen, W.S., Wu, C.K., Wong, K.L.: 'Inset microstripline-fed circularly polarized microstrip antennas', *IEEE Trans. Antennas Propag.*, 2000, **48**, (8), pp. 1253–1254